The AAPS Journal (2019) 21: 41
DOI: 10.1208/s12248-019-0311-4

Research Article

Effect of Dibasic Calcium Phosphate Incorporation on Cellulose Nanocrystal/Chitosan Hydrogel Properties for the Treatment of Vertebral Compression Fractures

Soheila Ali Akbari Ghavimi,[1] Ethan S. Lungren,[1] Jessica L. Stromsdorfer,[1] Blake T. Darkow,[1] Julie A. Nguyen,[1] Yisheng Sun,[1] Ferris M. Pfieffer,[1] Christina L. Goldstein,[2] Caixia Wan,[1] and Bret D. Ulery[1,3]

Received 17 December 2018; accepted 17 February 2019; published online 18 March 2019

Abstract. Vertebral compression fractures account for approximately 700,000 out of the 1.5 million total osteoporotic fractures that occur annually in the USA. There is growing interest in substituting currently utilized clinical treatments for vertebral compression fractures with an injectable, degradable, and bioactive system. In this research we studied the osteoinductive effect of calcium phosphate incorporation into cellulose nanocrystal/chitosan hydrogels with varying ratios of carbonate as an ionic crosslinker and genipin as a covalent crosslinker. As calcium and phosphate ions have been shown to be osteoinductive in time and concentration dependent manners, dibasic calcium phosphate was chosen as a bioactive additive due to its desirable controlled ion delivery potential. Gelation time, swelling ratio, erosion, compressive strength, and ion release behavior of different dibasic calcium phosphate incorporated hydrogels were evaluated. Mesenchymal stem cells were then exposed to mechanically competent hydrogels found capable of maintaining calcium and phosphate concentrations within the established bioactive range in order to assess their cytotoxicity and osteoinductivity. Our results demonstrate that hydrogels with higher covalent crosslinking possessed better mechanical properties and stabilities as well as more controlled calcium and phosphate ion release. Interestingly, dibasic calcium phosphate incorporation not only improved hydrogel bioactivity but also resulted in greater compressive strength.

KEY WORDS: vertebral compression fractures; hydrogel; chitosan; cellulose nanocrystals; calcium phosphate.

INTRODUCTION

Vertebral compression fractures (VCFs) are caused by the collapse of vertebral bone into itself which leads to sudden focal back pain and loss of function (1,2). Nearly three quarters of a million VCFs occur annually in the USA, primarily as a consequence of osteoporosis (3). Surgical interventions for VCFs normally consist of vertebroplasty or kyphoplasty (4–7), which involve modifying fractured bone tissue through the injection of poly(methylmethacrylate) (PMMA) bone cement into the vertebral body (8). PMMA is a non-bioactive, non-biodegradable polymer that possesses a much higher compressive strength than native bone tissue. While it is capable of treating the primary fracture, it leads to a significantly higher risk in the presentation of new fractures in patients treated with this material (9). Due to this limitation, novel approaches for the treatment of VCFs are greatly needed.

Chitosan hydrogels have been well studied as injectable, biodegradable, and bioactive systems for bone regenerative applications (10,11). One of the limitations of chitosan hydrogels for load bearing applications is their low compressive strength. This can be mitigated through compositing chitosan with other materials. Physical incorporation of cellulose nanocrystals (CNCs) (12,13) into chitosan hydrogels has been shown to enhance the mechanical properties of the resulting composite (CNC/chitosan) (14,15). CNC/chitosan hydrogels can be fabricated through physical association and/or chemical crosslinking of the chitosan cationic amine group. Previous research has shown that a higher swelling ratio, and more rapid degradability can be conveyed with ionic

Electronic supplementary material The online version of this article (https://doi.org/10.1208/s12248-019-0311-4) contains supplementary material, which is available to authorized users.

[1] Department of Biomedical, Biological, and Chemical Engineering, University of Missouri, Columbia, Missouri 65211, USA.
[2] Department of Orthopedic Surgery, University of Missouri, Columbia, Missouri, USA.
[3] To whom correspondence should be addressed. (e-mail: uleryb@missouri.edu)

crosslinking (16–18), whereas improved mechanical properties and chemical stability can be achieved through covalent crosslinking (16,17,19). Also, increased crosslinker density has been found to be correlated with hydrogel mechanical strength and stability (20,21).

An advantage of co-crosslinking CNC/chitosan hydrogels via both ionic and covalent methods is to allow for the fine tuning of the resulting material's physical and mechanical properties. Specifically, it is believed that through parameter optimization, a matrix capable of desirable bioactive reagent delivery for the treatment of VCFs can be achieved. Calcium phosphates (CaPs) are an excellent candidate as a bioactive additive due to their similar composition to natural bone (22) and intrinsic osteoinductivity (23). We have recently shown that mesenchymal stem cells (MSCs) exposed to sustained, appropriate concentrations of calcium (Ca^{2+}) and phosphate (P_i) ions facilitate their osteoblastic differentiation (24,25). The challenge with utilizing CaPs as bioactive fillers in CNC/chitosan hydrogels is regulating desirable ion release over time. The release rate of the ions in an aqueous environment depends on CaP dissolution kinetics and hydrogel matrix properties. The former can be regulated by different parameters such as nanocrystallinity and calcium/phosphate ratio (26,27), while the latter depends on hydrogel stability in the aqueous environment, which is directly related to crosslinking type and density (14).

In this research, we incorporated moderately decomposing dibasic CaP (24) into CNC/chitosan hydrogels bearing different crosslinking ratios for which CaP quantity was optimized in order to achieve suitable ion release profiles and appropriate hydrogel physical properties. Hydrogels with desirable ion release and material properties were exposed to mesenchymal stem cells to evaluate their cytotoxic and osteoinductive properties.

MATERIALS AND METHODS

Cellulose Nanocrystal Synthesis

Cellulose nanocrystals (CNCs) with no surface charge (^{0}CNCs) were obtained from cellulose microcrystals (CMCs, Avicel PH-101) as described elsewhere (14). Briefly, 3 g of CMCs was added to 150 mL of an acid solution consisting of 3 M citric acid and 6 M hydrochloric acid mixed together at a volumetric ratio of 9:1. The hydrolysis reaction was first conducted at 80 °C with continuous stirring for 4 h. Thereafter, the reaction mixture was transferred into dialysis tubes for processing in deionized (DI) water (28). The concentration of the CNC suspension was then adjusted to 0.1 wt% and pH adjusted to 10 with a NaOH solution. CTAB powder was added at a 1:2 M ratio of CNC carboxyl groups to CTAB to cap the carboxyl groups to yield ^{0}CNCs. This reaction was initiated at 60 °C for 3 h with continuous stirring and continued overnight at room temperature. A series of dialysis steps were then used to process the product until neutral pH was achieved.

Hydrogel Preparation

Low molecular weight chitosan (M_W ~ 50,000–190,000 Da; Sigma Aldrich) was dissolved in a 0.5% acetic acid in double-distilled water (ddH_2O) solution at 1.4% wt/v using constant magnetic stirring for 72 h at room temperature followed by vacuum filtration. ^{0}CNCs were suspended in the chitosan solution at 0.07% wt/v using 10 min of sonication employed with a probe-tip sonicator (Thermo Fisher) at 200 W. Dibasic calcium phosphate (DCP; Jost Chemical Co) was also suspended in the chitosan solution at 6% (DCP_6) and 10% (DCP_{10}) wt/v using the probe-tip sonicator at 200 W. Chitosan solutions without DCP were utilized as non-bioactive control groups. To prepare crosslinking solutions, sodium bicarbonate (ionic crosslinker) and genipin (covalent crosslinker) were dissolved in ddH_2O using the probe-tip sonicator at 200 W. The crosslinking solutions were created so that for each hydrogel, the molar ratio of crosslinker per deacetylated chitosan site (85% of total amines) was 5, 10, and 15 for sodium bicarbonate and 0.312, 1.25, and 2.5 for genipin. Hydrogels were fabricated by adding the appropriate crosslinking solution to a ^{0}CNC/DCP/chitosan solution and mixing using high-speed vortexing for 15 s. The samples were then placed in a water bath at 37 °C for further evaluation. Crosslinking solution combinations with ratios of 5:0.312:1, 5:1.25:1, 5:2.5:1, 10:0.312:1, 10:1.25:1, 10:2.5:1, 15:0.312:1, 15:1.25:1, or 15:2.5:1 of carbonate:genipin:chitosan (C:G:C) were evaluated.

Ion Release Study

Ca^{2+} and P_i release from DCP and hydrogels containing DCP was measured in ddH_2O at 37 °C over 14 days. Preformed hydrogels were immersed in water directly, and as a control, DCP powder was placed in a Transwell insert (Corning) and then immersed in water. At certain time points, ddH_2O was exchanged and the solution was saved for ion release measurement.

Calcium release was measured using the Calcium Liqui-Color Assay (Stanbio laboratory) following the manufacturer's protocol. In brief, the solution was diluted using a color and base reagent, mixed well, and read by a BioTek Cytation 5 fluorospectrometer plate reader at 550 nm. The absorbance was converted to Ca^{2+} content using a standard concentration curve in the linear range (0–15 mg/dL). Samples above the linear range were diluted with ddH_2O prior to being mixed with the color and base reagents.

Phosphate release was measured using the Phosphate Colorimetric Assay Kit (Sigma-Aldrich) according to the manufacturer's suggested procedure. In brief, the samples were mixed with phosphate reagent in a horizontal shaker and incubated at room temperature for 1 h while being protected from light. The absorbance was recorded at 650 nm with a BioTek Cytation 5 fluorospectrometer plate reader. The absorbance was converted to phosphate ion content using a standard curve in the linear range (0–5 nmol/mL). Samples above the linear range were diluted with ddH_2O prior to being mixed with the assay reagent.

Gelation Time Determination

Gelation time was determined using the tube inversion method (29). The hydrogel mixture was incubated in a plastic vial at 37 °C, which was then inverted every 30 s. The gelation time was recorded as the time that the mixture no longer

flowed and the vial could be completely inverted without the sample falling due to gravity.

Compressive Strength Assessment

Crosslinked cylindrical hydrogel disks with thickness of ~ 5 mm and diameter of ~ 10 mm were removed from their gelation vials. The mechanical properties of the samples were measured via compression tests using a TA Universal mechanical testing device. The strain response for each sample was monitored under a 5-kg load and a crosshead speed of 1 mm/min until 80% strain was achieved.

Swelling Measurement

Hydrogel swelling was assessed by first immersing samples in phosphate buffered saline (PBS) at 37 °C for 24 h. After 24 h, the samples were removed from PBS and blotted gently with Kimwipes to remove surface associated water after which they were weighed. The samples were then frozen at − 80 °C and lyophilized under vacuum (0.1 mmHg) and at − 50 °C for 72 h to make sure all solvent was removed. The samples were weighed after 3 days and the swelling ratio was measured using Eq. 1:

$$\text{Swelling} = \frac{W_\text{w}}{W_\text{d}} \tag{1}$$

where W_w is the wet hydrogel weight before lyophilization and W_d is the dry hydrogel weight after lyophilization.

Mass Loss Determination

Hydrogel mass loss was determined by immersing samples in PBS at 37 °C for a period of 14 days. At specific intervals, the samples were removed from PBS and blotted gently with Kimwipes to remove surface associated water after which they were weighed. Mass loss (%) was determined using Eq. 2:

$$\text{Mass Loss}\,(\%) = \frac{W_0 - \mathrm{W}_t}{W_0} \tag{2}$$

where W_0 and W_t are the initial weight and the weight at a specific time point, respectively. The endpoint data (i.e., day 14) are reported in this manuscript.

Cell Culture and Seeding

Murine mesenchymal stem cells (MSCs) were purchased from Cyagen, loaded into T-75 cell culture flasks (Corning), and grown at 37 °C in a humidified incubator with 5% CO_2 using growth media consisting of Dulbeco's modified Eagle's medium (DMEM, Invitrogen) supplemented with 10% fetal bovine serum (FBS, Invitrogen) and 1% penicillin–streptomycin (Pen-Strep, Invitrogen). Media was changed every 48 h until cells approached ~ 80% confluency after which they were dissociated using a 0.05% trypsin-EDTA solution (Invitrogen). Detached MSCs were counted using a hemocytometer and passed to new T-75 flasks at a splitting ratio of 1:4 or 1:5 dependent on overall cell count. After the fifth passage, cells were used for *in vitro* bioactivity studies. Tissue cultured polystyrene 24-well plates (Corning) were seeded with 30,000 cells/well and exposed to growth media alone as a negative control, ^{0}CNC/C:G:C hydrogels with different crosslinking ratios (5:1.25:1, 5:2.5:1, 10:2.5:1, 15:2.5:1) as potentially inert hydrogels or ^{0}CNC/DCP$_6$/C:G:C hydrogels with different crosslinking ratios (5:1.25:1, 5:2.5:1) or ^{0}CNC/DCP$_{10}$/C:G:C with different crosslinking ratios (5:2.5:1, 10:2.5:1, 15:2.5:1) as potentially bioactive hydrogels. MSCs were cultured for up to 14 days at 37 °C in a humidified incubator with 5% CO_2 for which growth media was changed every 3 days. Cell proliferation, viability, alkaline phosphatase (ALP) activity, and mineralization were assessed at 1, 3, 7, and 14 days.

Proliferation Assay

Cell proliferation was determined using the Quanti-iT PicoGreen dsDNA Assay (Thermo Fisher Scientific). At each end point, the samples were rinsed with PBS and exposed to 1% Triton X-100 (Sigma-Aldrich) followed by three freeze–thaw cycles in order to lyse the cells. Lysates were diluted with TE buffer (200 mM Tris-HCL, 20 mM EDTA, pH 7.5) and mixed with PicoGreen reagent according to the manufacturer's protocol. A BioTek Cytation 5 fluorospectrometer plate reader was utilized to measure the fluorescence of each sample (*ex.* 480 nm, *em.* 520 nm), and the cell number was determined using a MSC standard curve (0–200,000 cells/mL).

Viability Assay

Cell viability was evaluated at each time point using a MTS Cell Proliferation Colorimetric Assay Kit (BioVision). MTS reagent (20 μL) was added to growth media (500 μL) followed by 4 h incubation at 37 °C in a humidified incubator with 5% CO_2. Absorbance of each sample was measured at 490 nm. Cell viability was reported as the ratio of absorbance in the experimental groups compared to exposure to growth media alone as a negative control.

Alkaline Phosphatase Activity Assay

Cell ALP activity was quantified at each time point using an Alkaline Phosphatase Assay Kit (BioVision). In brief, 20 μL of cell lysate was combined with 50 μL of *p*-nitrophenyl phosphate (pNPP) solution in assay buffer. The mixture was incubated for 1 h at room temperature away from light. The reaction was stopped by the addition of 20 μL of stop solution and the absorbance of the resulting solution was measured at 405 nm using a plate reader. To eliminate any background effects, 1% Triton X-100 was incubated with pNPP, exposed to stop solution after 1 h, and its absorbance deducted from the value for each sample. The absorbance values were converted to the content of *p*-nitrophenyl (pNP) using a standard curve (0–20 nmol/mL) which was dephosphorylated using excess ALP enzyme. ALP activity was reported as pNP content normalized by cell count.

Mineralization Assay

Cell-based mineral deposition was measured at each time point using an Alizarin Red assay. At each time point, the media was removed after which the cells were washed with ddH_2O and fixed in 70% ethanol for 24 h. The ethanol was removed and the samples were incubated in 1 mL of 40 mM Alizarin Red solution (Sigma-Aldrich) for 10 min. The samples were rinsed with ddH_2O several times to ensure all non-absorbed stain was removed. Absorbed Alizarin Red was desorbed using 1 mL of a 10% cetylpyridinium chloride (CPC, Sigma-Aldrich) solution, after which stain concentration was measured at 550 nm using a plate reader. Absorbance of each sample was converted to the concentration of absorbed Alizarin Red using a standard curve (0–0.2740 mg/mL). Samples above the standard curve linear range were diluted with CPC until a solution in the linear range was obtained. Cell-based mineral deposition was calculated by subtracting mineralization found in blank wells exposed to the same experimental conditions. All results were normalized by cell count.

Statistical Analysis

JMP software was used to make comparisons between experimental groups with Tukey's HSD test specifically employed to determine pairwise statistical differences ($p < 0.05$). The statistical analysis results are reported in the supplemental information section. Groups that possess different letters have statistically significant differences in mean, whereas those that possess the same letter have means that are statistically insignificant in their differences.

RESULTS

Calcium and Phosphate Release from Cellulose Nanocrystal/Dibasic Calcium Phosphate/Carbonate:Genipin:Chitosan (^{0}CNC/DCP/C:G:C) Hydrogels

Ca^{2+} and P_i release profiles from DCP and hydrogels containing DCP are reported in Fig. I. DCP is a CaP with a relatively low K_{SP} that facilitates gradual dissolution and related ion release. In specific, DCP_6 (Fig. 1a, b) and DCP_{10} (Fig. 1c, d) released 21% and 22% of their total ion content, respectively, within 14 days. Both ^{0}CNC/DCP_6/C:G:C and ^{0}CNC/DCP_{10}/C:G:C hydrogels with the same crosslinking ratios showed similar ion release rates, indicating the differences in overall DCP content had neglectable influence on hydrogel ion release behavior. However, certain hydrogel formulations were found to retard the ion release rate for incorporated DCP. Specifically, the covalent crosslinking ratio was found to be quite important in ion release profile as the genipin content directly related to release rate (i.e., 14–19% for C:G:C X:0.3125:1, 9–12% for C:G:C X:1.25:1, and 5–8% for C:G:C X:2.5:1). In contrast, ionic crosslinker concentration made much less of an impact on ion release. The lowest ion release rate belongs to the hydrogel with the highest covalent and ionic crosslinker content (i.e., C:G:C 15:2.5:1) which was almost one fifth that of neat DCP (i.e., 5% compared to 22%).

Figure 2 represents the concentration of calcium and phosphate ion released from different materials after their immersion in water for 14 days for which the data was determined directly from the aforementioned ion release experiment (Fig. 1). As we have shown previously, calcium ion concentrations of 1–16 mM and phosphate ion concentrations of 1–8 mM were successfully able to induce mesenchymal stem cell (MSC) osteogenic differentiation without being cytotoxic (24). As shown in Fig. 2a, b, ^{0}CNC/DCP_6/C:G:C hydrogels showed desirable controlled ion release properties with formulations maintaining the therapeutic window of calcium and all hydrogels except C:G:C 5:0.312:1, 10:0.312:1, and 15:0.312:1 as well as DCP itself achieving phosphate release in the therapeutic window. In contrast, ^{0}CNC/DCP_{10}/C:G:C hydrogels showed less desirable controlled release profiles, with only C:G:C 15:1.25:1 and 15:2.5:1 maintaining the release of both ions within their respective therapeutic windows.

Materials Properties of Cellulose Nanocrystal/Dibasic Calcium Phosphate/Carbonate:Genipin:Chitosan (^{0}CNC/DCP/C:G:C) Hydrogels

Gelation times for different ^{0}CNC/DCP/chitosan hydrogels are shown in Fig. 3. Incorporation of DCP decreased gelation time, however, the amount of DCP content did not have a noticeable impact. Also, increasing genipin content for all ^{0}CNC/DCP/chitosan hydrogels was found to decrease the gelation time. For hydrogels without DCP, genipin content decreased the gelation time of hydrogels with lower carbonate content (i.e., C:G:C 5:X:1 and C:G:C 10:X:1), but it did not change the gelation time for higher carbonate content (i.e., C:G:C 15:X:1). Carbonate content was found to impact gelation time for all hydrogels regardless of DCP incorporation and content with the greatest impact seen with the lowest covalent crosslinking ratio (i.e., C:G:C X:0.312:1).

The swelling ratio and mass loss of ^{0}CNC/DCP/chitosan hydrogels are reported in Table I for which statistical analysis was conducted to determine the impact of ionic crosslinking ratio (Table S1), covalent crosslinking ratio (Table S2), and DCP incorporation (Table S3). DCP incorporation decreases the hydrogel swelling ratio dramatically. The swelling ratio for ^{0}CNC/chitosan hydrogels was found to be 17–28, while it was only 5–7 for hydrogels containing DCP. Increased DCP content also slightly decreased the swelling ratio. The hydrogel swelling ratio also varied slightly as a function of crosslinker quantity. Increasing hydrogel carbonate or genipin content caused a slight decrease in hydrogel swelling. Hydrogel mass loss at 14 days decreased approximately 10% when DCP was incorporated regardless of the amount added (i.e., 45–35% for ^{0}CNC/C:G:C hydrogels and 39–21% for ^{0}CNC/DCP/C:G:C hydrogels). Ionic and covalent crosslinking did not dramatically alter hydrogel mass loss over 14 days.

The compressive strength of ^{0}CNC/DCP/C:G:C hydrogels is detailed in Fig. 4 for which statistical analysis was conducted to determine the impact of ionic crosslinking ratio (Table S4), covalent crosslinking ratio (Table S5), and DCP incorporation (Table S6). DCP incorporation significantly increased hydrogel compressive strength with the greatest impact found with low carbonate content hydrogels

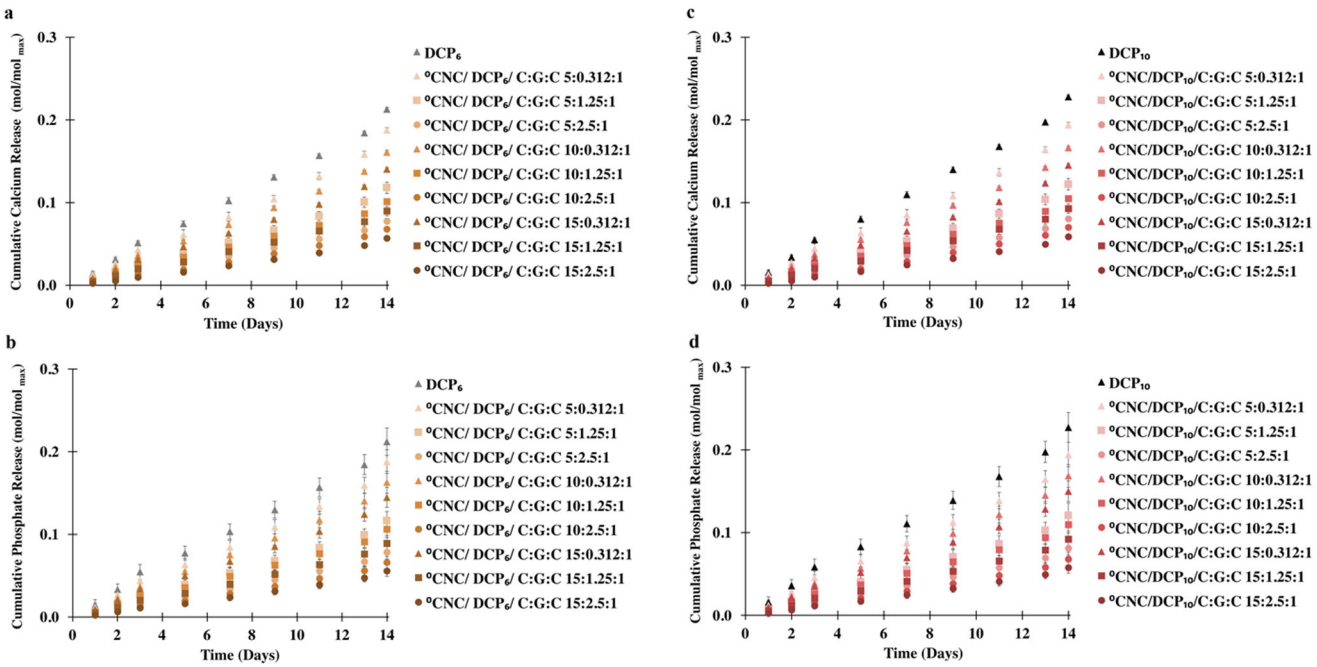

Fig. 1. Cumulative calcium and phosphate ion release. **a** Ca^{2+} and **b** P_i release from ^{0}CNC/DCP$_6$/C:G:C hydrogels as well as **c** Ca^{2+} and **d** P_i release from ^{0}CNC/DCP$_{10}$/C:G:C hydrogels was measured for hydrogels that were immersed in ddH_2O for 14 days at 37 °C. The cumulative data were normalized by maximum ion content for each material ($N = 4$)

(i.e., C:G:C 5:X:1). Higher DCP content (DCP$_{10}$) showed further improvement in hydrogel compressive strength when compared to lower DCP content (DCP$_6$). The compressive strength of ^{0}CNC/C:G:C hydrogels without DCP was not significantly influenced by changes in carbonate or genipin content. However, in ^{0}CNC/DCP/C:G:C hydrogels, the lowest carbonate containing formulations (i.e., C:G:C 5:X:1) showed statistically significant increases in compressive strength. The greatest compressive strength observed among all of the different formulations evaluated was 324 kPa which was achieved with ^{0}CNC/DCP$_{10}$/C:G:C 5:1.25:1 hydrogels.

Bioactivity of Cellulose Nanocrystal/Dibasic Calcium Phosphate/Carbonate:Genipin:Chitosan (^{0}CNC/DCP/C:G:C) Hydrogels

As ^{0}CNC/C:G:C hydrogels were being designed for VCF repair applications, their impact on mesenchymal stem cell

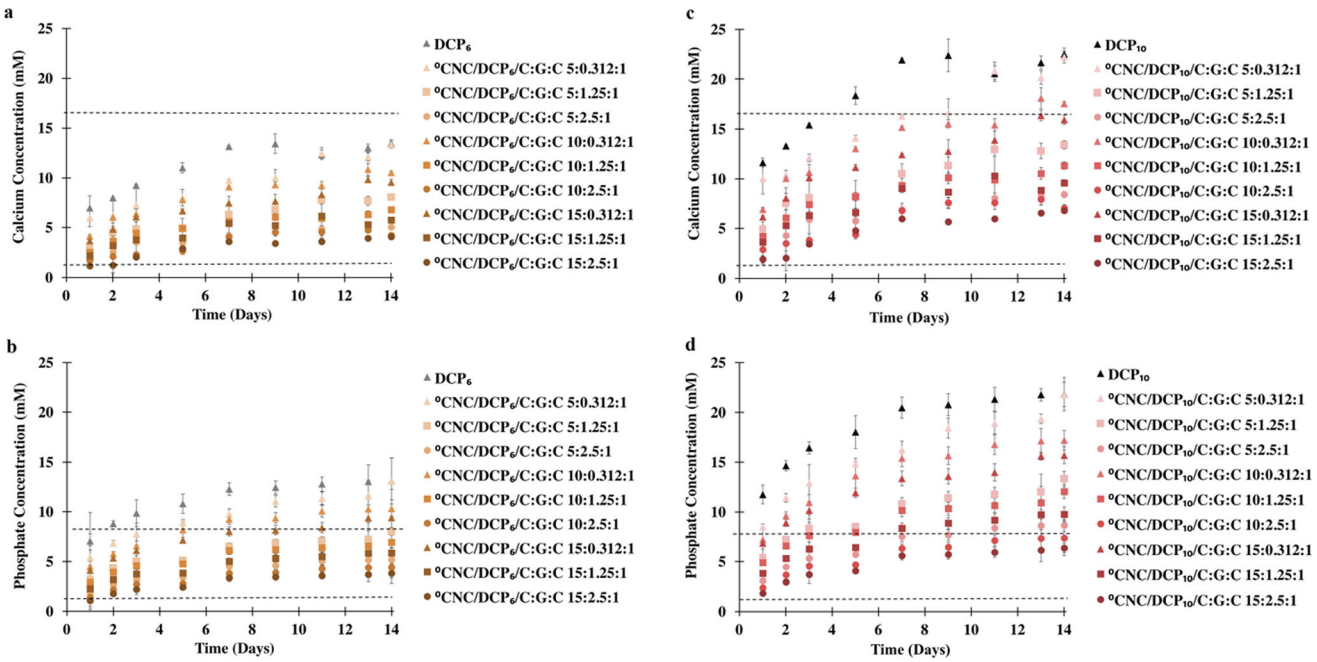

Fig. 2. Released calcium and phosphate ion concentration. **a** Ca^{2+} and **b** P_i release from ^{0}CNC/DCP$_6$/C:G:C hydrogels as well as **c** Ca^{2+} and **d** P_i release from ^{0}CNC/DCP$_{10}$/C:G:C hydrogels was measured for hydrogels that were immersed in ddH_2O for 14 days at 37 °C ($N = 4$)

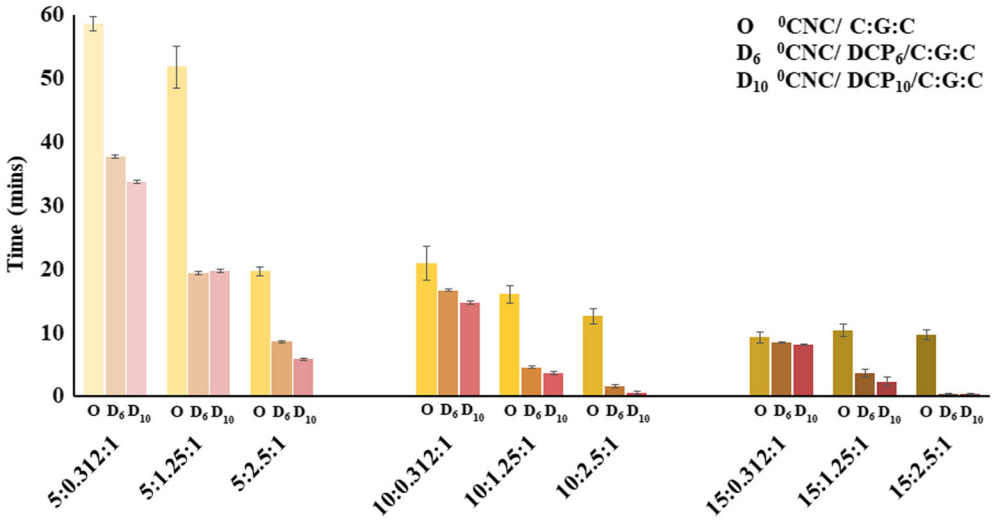

Fig. 3. Gelation time for ^{0}CNC/C:G:C hydrogels with varying crosslinking ratios and DCP incorporation. Hydrogels were prepared without DCP (O), with 6% DCP (D_6), and 10% DCP (D_{10}). The inversion method at 37 °C was used to determine in situ gelation time. Results are an average of four independent measurements

(MSC) health and osteogenesis needed to be explored. The choice of hydrogels used in these biological experiments were made based on their capacity to maintain calcium and phosphate ion release within the osteoinductive therapeutic window for 14 days while possessing a compressive strength of at least 120 kPa. Based on this criteria, five DCP containing formulations (i.e., ^{0}CNC/DCP_6/C:G:C 5:1.25:1 and 5:2.5:1, and ^{0}CNC/DCP_{10}/C:G:C 5:2.5:1, 10:2.5:1, and 15:2.5:1) were studied further. ^{0}CNC/C:G:C 5:1.25, 5:2.5:1, 10:2.5:1, and 15:2.5:1 were evaluated as biologically inert controls to determine the impact calcium and phosphate ion release had on hydrogel cytotoxicity and inductivity. Neat DCP was also included to investigate the impact of controlled ion release on stem cell behavior. MSC proliferation and viability due to the presence of different hydrogel formulations are shown in Fig. 5, for which statistical analysis was conducted to assess the impact of formulation (Table S4) and time (Table S5). MSCs seeded on tissue cultured plastic (Ctrl) and incubated in growth media proliferated to seven times initial seeding cell number over 14 days of culture (Fig. 5a). In contrast, MSCs exposed to any hydrogel formulation showed some decrease in cell count in the first day followed by either remaining at a constant amount throughout the rest of the 14 days of the experiment for ^{0}CNC/chitosan hydrogels or proliferating slightly (i.e., up to two times of initial seeding) for ^{0}CNC/DCP/chitosan hydrogels (Fig. 5a). The number of cells exposed to DCP_6 slightly decreased at day 1 to 75% initial seeding followed by an increase to 50% initial seeding by day 3 and after while the decrease in cell number exposed to DCP_{10} was up to 25% at day 1 and remained constant afterward. At each time point, MSCs given growth media alone (Ctrl) were found to be at statistically significantly greater cell counts than all hydrogel formulations and cells exposed to ^{0}CNC/DCP/C:G:C hydrogels maintained statistically significantly greater numbers than ^{0}CNC/C:G:C hydrogels and DCP alone (Table S4). A MTS assay showed that MSCs exposed to any ^{0}CNC/C:G:C hydrogel formulation as well as DCP for up to 14 days were more than 50%

Table I. Swelling Ratio and Mass Loss for C:G:C Hydrogels with Different Crosslinking Ratios and DCP Incorporation. The Swelling Ratio Was Determined as the Ratio of Wet Weight to Dry Weight of Hydrogels After Immersion in PBS for 24 h at 37 °C. Mass Loss Was Measured by Immersing Hydrogels in PBS at 37 °C for 14 Days and Comparing the Change in Mass Over Time. Results Are the Averages of Four Independent Measurements

C:G:C	^{0}CNC		^{0}CNC/DCP_6		^{0}CNC/DCP_{10}	
	Swelling ratio	Mass loss (%)	Swelling ratio	Mass loss (%)	Swelling ratio	Mass loss (%)
5:0.312:1	28.7 ± 1.3	45.4 ± 2.1	7.1 ± 0.2	37.3 ± 1.9	6.8 ± 0.5	39.4 ± 5.2
5:1.25:1	25.8 ± 2.1	42.8 ± 5.9	6.8 ± 0.2	33.5 ± 7.1	6.0 ± 0.3	34.6 ± 7.7
5:2.5:1	19.8 ± 1.4	37.0 ± 3.4	5.6 ± 0.1	31.0 ± 4.9	4.7 ± 1.0	30.5 ± 13.8
10:0.312:1	25.3 ± 3.3	40.5 ± 5.4	6.7 ± 0.3	36.7 ± 6.7	6.6 ± 0.3	38.6 ± 7.3
10:1.25:1	22.7 ± 3.3	38.0 ± 10.6	6.2 ± 0.2	33.6 ± 8.3	5.7 ± 0.8	33.8 ± 10.4
10:2.5:1	18.0 ± 1.6	35.5 ± 9.6	5.5 ± 0.2	29.9 ± 5.2	5.3 ± 0.4	29.9 ± 8.7
15:0.312:1	23.6 ± 2.3	43.8 ± 5.9	6.2 ± 1.3	32.9 ± 1.9	6.2 ± 2.4	37.8 ± 7.4
15:1.25:1	21.3 ± 0.4	39.7 ± 16.1	5.5 ± 1.3	22.5 ± 7.4	5.3 ± 1.1	32.9 ± 5.9
15:2.5:1	16.9 ± 1.8	34.3 ± 12.9	5.3 ± 0.9	21.5 ± 9.4	5.2 ± 0.3	23.6 ± 8.4

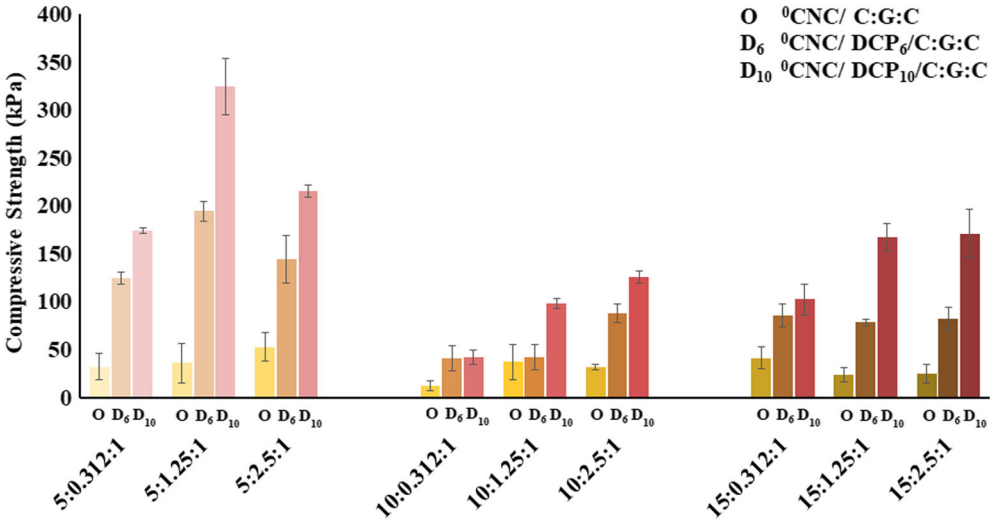

Fig. 4. Compressive strength for ^{0}CNC/C:G:C hydrogels with different crosslinking ratios and DCP incorporation. Hydrogels were prepared without DCP (O), with 6% DCP (D_6), and 10% DCP (D_{10}). Results are the average of four independent measurements. Statistical analysis of the differences between groups is available in supplementary information (Table S4, Table S5, and Table S6)

metabolically active compared to the control treatment (Fig. 5b). No statistically significant differences in viability were observed among any ^{0}CNC/C:G:C hydrogel groups or time points (Table S4 and Table S5). MSCs exposed to ^{0}CNC/DCP/C:G:C hydrogels showed more than 80% metabolic activity compared within 14 days compared to the control treatment. The difference between viability of the MSCs exposed to ^{0}CNC/DCP/C:G:C were statistically significantly greater than ^{0}CNC/DCP/chitosan hydrogels and DCP for all time points (Table S5). Interestingly, neither crosslinker type (i.e., ionic or covalent) nor crosslinker ratio was found to dramatically impact MSC proliferation or viability.

MSC ALP activity and mineralization due to interactions with different hydrogel formulations are provided in Fig. 6, for which statistical analysis is provided (Table S4 and Table S5). MSCs exposed to media alone (Ctrl) showed background levels of ALP expression, which were statistically significantly lower than any ^{0}CNC/C:G:C hydrogels, any ^{0}CNC/DCP/C:G:C hydrogels, and both DCPs at each time point (Fig. 6a; Table S4). Furthermore, MSCs cultured with ^{0}CNC/DCP/C:G:C hydrogels had statistically higher ALP activity than those presented with their respective ^{0}CNC/C:G:C hydrogels at days 7 and 14 (Fig. 6a; Table S4). Controlled ion release from any of the ^{0}CNC/DCP_{10}/C:G:C hydrogels caused statistically significant increased cell-based ALP activity compared to DCP_{10} at days 7 and 14 (Fig. 6a; Table S4). MSCs exposed to ^{0}CNC/DCP_{10}/C:G:C 15:2.5:1 also showed higher ALP activity compared to cells cultured with ^{0}CNC/DCP_6/C:G:C 5:1.25:1 and ^{0}CNC/DCP_6/C:G:C 5:2.5:1 at day 14 (Fig. 6a; Table S4). MSC mineralization evaluation revealed similar trends to the ALP activity data (Fig. 6b). By day 7, the presence of any DCP or hydrogel containing DCP yielded an increase in cell-based mineral deposition compared to the Ctrl group (Fig. 6b; Table S4). Controlled ion release from ^{0}CNC/DCP_{10}/C:G:C 10:2.5:1 and 15:2.5:1 hydrogels caused statistically significant cell-based mineralization than DCP_{10} at day 7 and 14 (Fig. 6a; Table S4). Additionally, MSCs exposed to ^{0}CNC/DCP_{10}/C:G:C 10:2.5:1 and 15:2.5:1 showed slightly higher levels of mineralization compared to cells cultured with ^{0}CNC/DCP_6/C:G:C 5:1.25:1, ^{0}CNC/DCP_6/C:G:C 5:2.5:1, and ^{0}CNC/DCP_{10}/C:G:C 5:2.5:1 formulations for days 3, 7, and 14 though the differences were found to be statistically insignificant (Fig. 6b; Table S4).

DISCUSSION

The goal of our current research was to design an injectable bioactive hydrogel capable of stimulating bone remodeling. CaPs are an attractive candidate as a bioactive additive since they mimic the inorganic phase of natural bone and are inherently bioactive (22). The enclosed hydrogel system has been designed to be injectable and capable of undergoing in situ gelation allowing it to be useful for minimally invasive procedures which is not possible with solid scaffold materials (25,30). Also, our composite hydrogel's mechanical properties and stability better mimic native bone better than other injectable materials such as PMMA, calcium phosphate, calcium sulfate cement (31), and other softer hydrogels (32–34). Interestingly, the addition of DCP as a bioactive component enhances material processability and reduces cost compared to scaffolds for which growth factor incorporation has been used to convey osteoinductivity (35).

The osteoinductive properties of CaPs have been shown to be dependent on their total concentration and controlled release of their calcium and phosphate ions (23,25). Based on the ion release results (Figs. 1 and 2), increasing the ratio of both ionic and covalent crosslinker in ^{0}CNC/DCP/C:G:C hydrogels led to a decrease in the ion release rate compared to DCP alone. This behavior can be attributed to physical entanglement and entrapment of the dibasic calcium phosphate within the chitosan matrix due to increased crosslinker density shortening the average crosslink distance (36), which decreases the pore size in the polymeric network and hinders ion diffusion (37,38). The effect of genipin content was found to be more significant than carbonate content, which is unsurprising, as covalent crosslinker is less flexible than physical, ionic crosslinking (39). ^{0}CNC/DCP_6/C:G:C X:2.5:1 and X:1.25:1 as well as ^{0}CNC/DCP_{10}/C:G:C

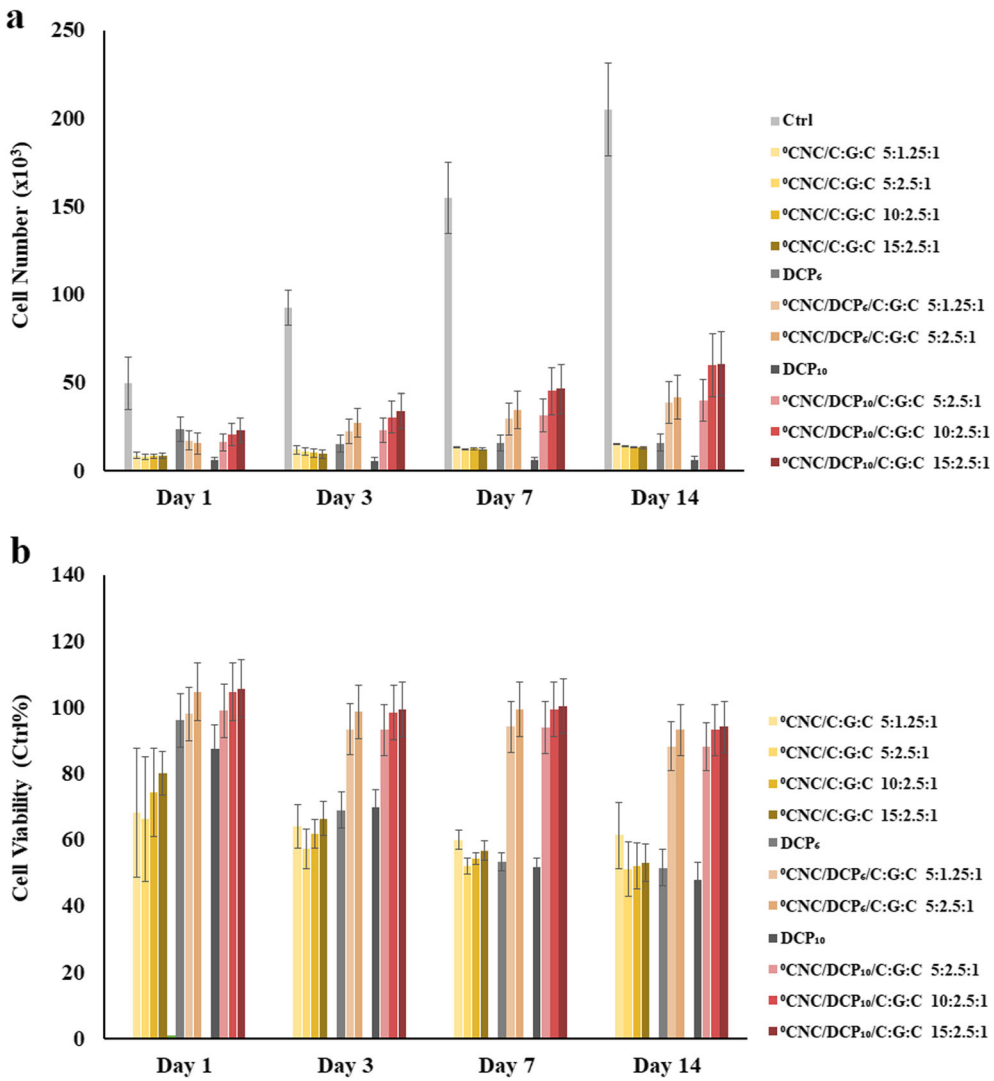

Fig. 5. Health of MSCs exposed to ^{0}CNC/C:G:C hydrogels with different crosslinking ratios and DCP incorporation. MSC **a** proliferation and **b** viability were measured for cells cultured with different materials in growth media for 14 days at 37 °C. Cell count was measured by the Quanti-iT PicoGreen Assay with or without ^{0}CNC/C:G:C or ^{0}CNC/DCP/C:G:C hydrogels with different crosslinking ratios ($N = 4$). Cell metabolism was indirectly evaluated by NAD(P)H activity using a MTS assay with or without ^{0}CNC/C:G:C or ^{0}CNC/DCP/C:G:C hydrogels with different crosslinking ratios ($N = 4$). Statistical analysis of the differences between groups and time points is available in supplementary information (Table S4 and Table S5)

15:2.5:1 and ^{0}CNC/DCP$_{10}$/C:G:C 15:1.25:1 were capable of maintaining the Ca^{2+} and P_i concentration within the therapeutic window (i.e., non-cytotoxic and inductive range - 1 mM ≤ Ca^{2+} ≤ 16 mM and 1 mM ≤ P_i ≤ 8 mM) (24) (Fig. 2). These results confirm that a versatile hydrogel network can be developed with the capacity to achieve desirable release profiles of different loading concentrations of bioactive reagents.

DCP incorporation also yielded decreased hydrogel gelation times, with the most significant changes observed in hydrogels with the lowest carbonate content (i.e., 5:X:1) (Fig. 3). These observations can be attributed to the formation of additional complexes or reversible ionic crosslinks between the phosphate content of DCP and chitosan (40), which increased crosslinking density and led to decreased gelation time (41,42). Since localized charge density is lowest in hydrogels with the lowest carbonate content, the most significant decreases in gelation time due to this impact can be observed with these materials. Ideally, hydrogels should undergo fast gelation (< 20 min) to limit surgery-related infection risks and efficiently fill the defect site (43). According to our results, all hydrogels except those with C:G:C 5:0.312:1 can be formed before the ideal time limit.

DCP incorporation showed a noticeable decrease in hydrogel swelling ratio and slight improvement in stability (i.e., ~ 10% less mass loss; Table I). These observations are likely due to the synergistic effects of charge density and physical density. The increased ionic crosslinks provided by the presence of DCP limit hydrogel molecular rearrangement, thus restricting water infiltration-related expansion (40). Also, the presence of DCP in the same chitosan hydrogel volume increases overall material density limiting

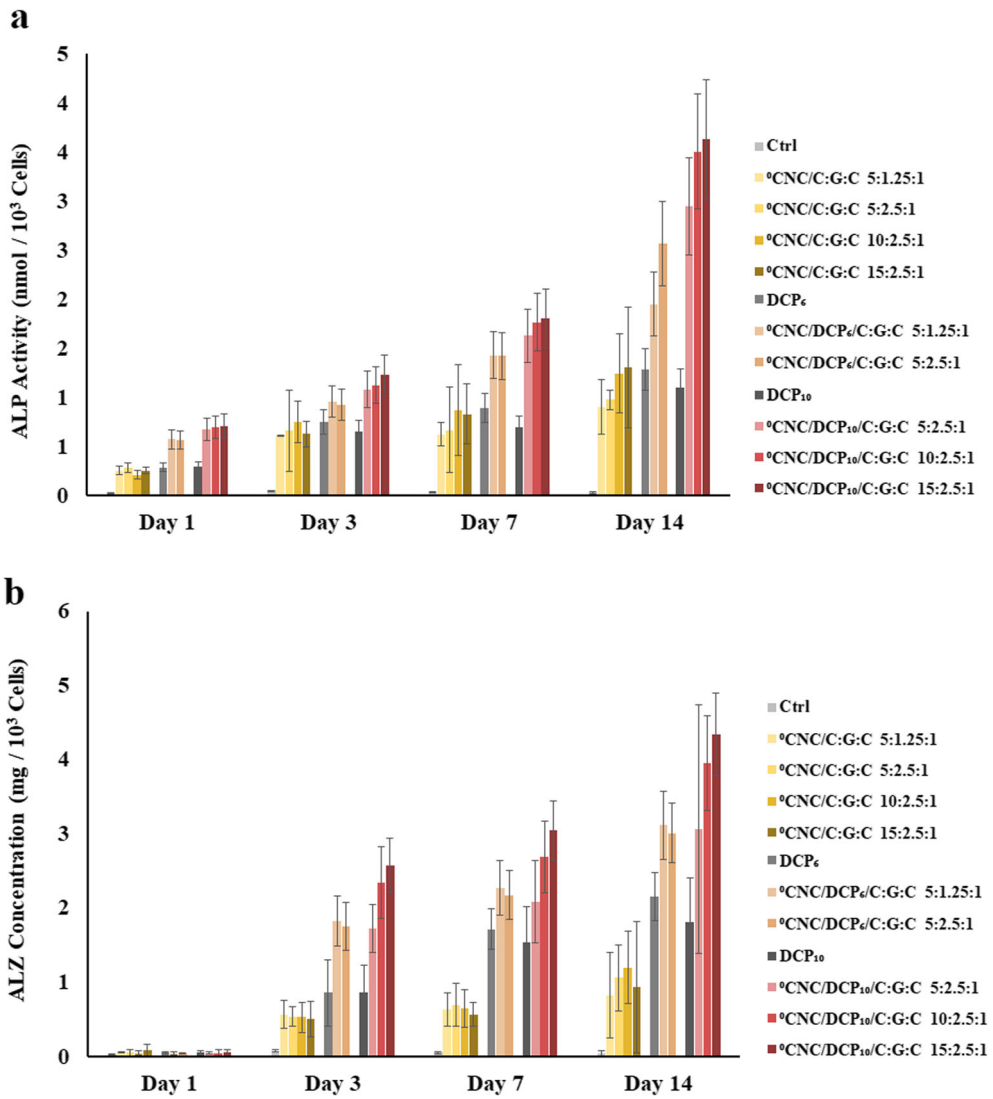

Fig. 6. Differentiation of MSCs exposed to ^{0}CNC/C:G:C hydrogels with different crosslinking ratios and DCP incorporation. MSC alkaline phosphatase (ALP) activity (**a**) and cell-based mineralization (**b**) of MSCs cultured with different materials in growth media for 14 days at 37 °C. Cell ALP enzyme activity was analyzed by an ALP Assay with or without ^{0}CNC/C:G:C or ^{0}CNC/DCP/C:G:C hydrogels with different crosslinking ratios ($N = 4$). Alizarin red (ALZ) staining was used as an indirect measure of mineralization with and without ^{0}CNC/C:G:C or ^{0}CNC/DCP/C:G:C hydrogels with different ionic crosslinkers and crosslinking ratios ($N = 4$). ALZ content for matching acellular hydrogel formulation over the same incubation time was subtracted to determine cell-based mineralization. ALP activity and mineralization were normalized on a per cell basis, and statistical analysis between groups and time points is available in supplementary information (Table S4 and Table S5)

the physical space for which water can penetrate, swell the hydrogel, and lead to matrix erosion (36–38).

Enhanced mechanical properties were observed in all DCP incorporated hydrogel formulations for which higher compressive strength correlated with greater DCP content (Fig. 4). DCP incorporation in the lowest carbonate content (i.e., 5:X:1) hydrogels facilitated the most significant improvement in compressive strength compared to the higher carbonate content hydrogels (Fig. 4). Due to their high compressive strength and moduli, CaPs have been widely used as polymer matrix fillers capable of yielding composites with highly desirable mechanical properties (44–47). A major factor affecting the physical properties of the polymer/CaP composites is their interfacial stability. Due to the significant differences between hydrophobic polymers and CaPs, their composites can often be weaker and less stable (48). However, in the case of the hydrophilic ^{0}CNC/ C:G:C matrix, the ionic bonding between the phosphate content of DCP and the amine sites in chitosan can lead to efficient interactions at the component interface, leading to greater compressive strength of the resulting composite. This phenomenon was best observed when DCP was incorporated within the lowest carbonate content hydrogels. This is believed to have been caused by a higher density of DCP/chitosan ionic interactions rather than higher carbonate content hydrogels due to fewer carbonate ions available to

compete for complexation (49). Ideally, the mechanical properties of hydrogels intended for VCF repair applications should approach those of the human vertebrae (compressive strength for healthy adults range from 0.6 to 6 MPa (50) and osteoporotic vertebrae, which are 25 to 35% weaker (51)). Our results indicate that ^{0}CNC/DCP_6/C:G:C 5:0.312:1, 5:1.25:1, 5:2.5:1, and ^{0}CNC/DCP_{10}/C:G:C 5:0.312:1, 5:1.25:1, 5:2.5:1, 10:2.5:1, 15:1.25:1, 15:2.5:1 can all potentially be candidates for the treatment of VCFs due to their sufficient compressive strength (Fig. 4).

While enhanced hydrogel mechanical competency is an attractive feature, the primary rationale for DCP incorporation into ^{0}CNC/C:G:C hydrogels was to improve their bioactivity. Therefore, hydrogels with the ability to control Ca^{2+} and P_i release while possessing sufficient compressive strength and gelation time (^{0}CNC/DCP_6/C:G:C 5:1.25:1 and 5:2.5:1 as well as ^{0}CNC/DCP_{10}/C:G:C 5:2.5:1, 10:2.5:1, and 15:2.5:1) were further assessed by a cell study. Our results showed that DCP incorporation moderated the initial decrease in MSC cell number to ~ 75% of initial seeded cell count with ^{0}CNC/DCP/chitosan hydrogels compared to ~ 25% of initial seeded cell count observed with ^{0}CNC/chitosan hydrogels (Fig. 5). The decrease in cell number in the first day of culturing can be attributed to the influence of hydrogel components (52–54), mechanotransduction (55,56), and pH (57,58) on cells during their initial contact with hydrogels. Incorporation of DCP into the hydrogels enhanced the MSC response to the hydrogels due to the desirable effect Ca^{2+} and P_i have on MSC growth and viability (25,59,60), as well as the environment pH (basic carbonate and acidic CaP can neutralize one another). Interestingly, the presence of DCP_6 and DCP_{10} yielded lower cell numbers than DCP incorporated hydrogels likely due to higher concentration of Ca^{2+} and P_i generated from the uninhibited neat CaPs (24). While sudden cell death was found at day 1 for MSCs due to the presence of ^{0}CNC/C:G:C hydrogels, cell count remained stable for the rest of the experiment. In contrast, MSCs exposed to ^{0}CNC/DCP/C:G:C hydrogels grew statistically significantly over the 14 days of the study. Due to the presence of ^{0}CNC/DCP/C:G:C hydrogels, cell numbers were still lower than the control group, though this could have been due to the fact that MSC differentiation decreases their proliferative capacity. MTS results that showed a statistically significant improvement in the viability of MSCs exposed to the DCP incorporated hydrogels though cells that survived initial exposure to ^{0}CNC/C:G:C hydrogels were found to be ~ 60% viable throughout the study as well. MSCs cultured with ^{0}CNC/DCP/C:G:C hydrogels excitingly showed statistically significant greater ALP activity (an early marker for osteoblast differentiation) than those incubated with neat DCP or ^{0}CNC/C:G:C hydrogels (Fig. 6a). Furthermore, statistically significant enhanced osseous mineralization (a late marker for osteoblast differentiation) was observed for MSCs exposed to the same hydrogel formulations (Fig. 6b). Hydrogels with 10% DCP induced slightly higher ALP activity and mineralization than 6% DCP incorporated hydrogels, likely due to modestly higher Ca^{2+} and P_i release (closer to the upper boundary of their therapeutic window; Fig. 2).

CONCLUSION

This research detailed an injectable chitosan-based hydrogel system with cellulose nanocrystals as a reinforcing reagent, carbonate, and genipin as ionic and covalent crosslinkers, respectively, and dibasic calcium phosphate as a bioactive additive. Co-crosslinking yielded hydrogels that can control the release of inductive calcium and phosphate ions, as well as offered a tunable system that can be readily modified for a variety of future applications. The incorporation of dibasic calcium phosphate decreased the gelation time, the swelling ratio, and the mass loss of hydrogels, as well as improved their compressive strength. Additionally, dibasic calcium phosphate moderated the cytotoxic effect of cellulose nanocrystal/chitosan hydrogels and induced significant osteogenic differentiation of mesenchymal stem cells. The resulting composite hydrogel represents a novel biomaterial with desirable processing, mechanical, and bioactive properties, making it an attractive candidate for treating vertebral compression fractures in osteoporotic patients.

ACKNOWLEDGMENTS

The authors gratefully acknowledge support from the Coulter Translational Partnership Program at the University of Missouri.

FUNDING INFORMATION

Start-up funds are provided by the University of Missouri.

REFERENCES

1. Ensrud KE, Schousboe JT. Vertebral fractures. N Engl J Med. 2011;364(17):1634–42.
2. Wong CC, McGirt MJ. Vertebral compression fractures: a review of current management and multimodal therapy. J Multidiscip Healthc. 2013;6:205.
3. Ferrone ML, Schoenfeld AJ. Osteoporosis, vertebral compression fractures, and cement augmentation procedures. In: Principles of orthopedic practice for primary care providers. Springer; 2018. p. 63–72.
4. McGirt MJ, Parker SL, Wolinsky J-P, Witham TF, Bydon A, Gokaslan ZL. Vertebroplasty and kyphoplasty for the treatment of vertebral compression fractures: an evidenced-based review of the literature. Spine J. 2009;9(6):501–8.
5. De Negri P, Tirri T, Paternoster G, Modano P. Treatment of painful osteoporotic or traumatic vertebral compression fractures by percutaneous vertebral augmentation procedures: a nonrandomized comparison between vertebroplasty and kyphoplasty. Clin J Pain. 2007;23(5):425–30.
6. Hadjipavlou A, Tzermiadianos M, Katonis P, Szpalski M. Percutaneous vertebroplasty and balloon kyphoplasty for the treatment of osteoporotic vertebral compression fractures and osteolytic tumours. Bone Joint J. 2005;87(12):1595–604.
7. Watts N, Harris S, Genant H. Treatment of painful osteoporotic vertebral fractures with percutaneous vertebroplasty or kyphoplasty. Osteoporos Int. 2001;12(6):429–37.
8. Denaro V, Longo UG, Maffulli N, Denaro L. Vertebroplasty and kyphoplasty. Clin Cases Min Bone Metab. 2009;6(2):125–30.
9. Ali U, Karim KJBA, Buang NA. A review of the properties and applications of poly (methyl methacrylate) (PMMA). Polym Rev. 2015;55(4):678–705.
10. Levengood SKL, Zhang M. Chitosan-based scaffolds for bone tissue engineering. J Mater Chem B. 2014;2(21):3161–84.
11. Liu M, Zeng X, Ma C, Yi H, Ali Z, Mou X, *et al*. Injectable hydrogels for cartilage and bone tissue engineering. Bone Res. 2017;5:17014.

12. Yang J, Han C-R, Duan J-F, Ma M-G, Zhang X-M, Xu F, *et al*. Studies on the properties and formation mechanism of flexible nanocomposite hydrogels from cellulose nanocrystals and poly (acrylic acid). J Mater Chem. 2012;22(42):22467–80.
13. Yang X, Bakaic E, Hoare T, Cranston ED. Injectable polysaccharide hydrogels reinforced with cellulose nanocrystals: morphology, rheology, degradation, and cytotoxicity. Biomacromolecules. 2013;14(12):4447–55.
14. Soheila Aliakbari Ghavimi ESL, Faulkner TJ, Josselet MA, Wu Y, Sun Y, Pfeiffer FM, Goldstein CL, Wan C, Ulery BD. Inductive co-crosslinking of cellulose nanocrystals/chitosan hydrogels for treatment of vertebral compression fractures. Submitted. 2018.
15. HPS AK, Saurabh CK, Adnan A, Fazita MN, Syakir M, Davoudpour Y, *et al*. A review on chitosan-cellulose blends and nanocellulose reinforced chitosan biocomposites: properties and their applications. Carbohydr Polym. 2016;150:216–26.
16. Berger J, Reist M, Mayer JM, Felt O, Peppas N, Gurny R. Structure and interactions in covalently and ionically crosslinked chitosan hydrogels for biomedical applications. Eur J Pharm Biopharm. 2004;57(1):19–34.
17. Moura MJ, Faneca H, Lima MP, Gil MH, Figueiredo MM. In situ forming chitosan hydrogels prepared via ionic/covalent co-cross-linking. Biomacromolecules. 2011;12(9):3275–84.
18. Adekogbe I, Ghanem A. Fabrication and characterization of DTBP-crosslinked chitosan scaffolds for skin tissue engineering. Biomaterials. 2005;26(35):7241–50.
19. Mi F-L, Tan Y-C, Liang H-C, Huang R-N, Sung H-W. In vitro evaluation of a chitosan membrane cross-linked with genipin. J Biomater Sci Polym Ed. 2001;12(8):835–50.
20. Lee KY, Rowley JA, Eiselt P, Moy EM, Bouhadir KH, Mooney DJ. Controlling mechanical and swelling properties of alginate hydrogels independently by cross-linker type and cross-linking density. Macromolecules. 2000;33(11):4291–4.
21. Bhattarai N, Gunn J, Zhang M. Chitosan-based hydrogels for controlled, localized drug delivery. Adv Drug Deliv Rev. 2010;62(1):83–99.
22. Liao S, Cui F, Zhang W, Feng Q. Hierarchically biomimetic bone scaffold materials: nano-HA/collagen/PLA composite. J Biomed Mater Res B Appl Biomater. 2004;69(2):158–65.
23. Cushnie EK, Ulery BD, Nelson SJ, Deng M, Lo KW, Khan YM, *et al*. Simple signaling molecules for inductive bone regenerative engineering. 2014.
24. Ghavimi SAA, Allen BN, Stromsdorfer JL, Kramer JS, Li X, Ulery B. Calcium and phosphate ions as simple signaling molecules with versatile osteoinductivity. Biomedical Materials. 2018.
25. Ghavimi SAA, Tata RR, Greenwald AJ, Allen BN, Grant DA, Grant SA, *et al*. Controlled ion release from novel polyester/ceramic composites enhances osteoinductivity. AAPS J. 2017;1–16.
26. Ducheyne P, Radin S, King L. The effect of calcium phosphate ceramic composition and structure on in vitro behavior. I. Dissolution. J Biomed Mater Res. 1993;27(1):25–34.
27. Vallet-Regí M, González-Calbet JM. Calcium phosphates as substitution of bone tissues. Prog Solid State Chem. 2004;32(1):1–31.
28. Yu H-Y, Zhang D-Z, Lu F-F, Yao J. New approach for single-step extraction of carboxylated cellulose nanocrystals for their use as adsorbents and flocculants. ACS Sustain Chem Eng. 2016;4(5):2632–43.
29. Nair LS, Starnes T, Ko J-WK, Laurencin CT. Development of injectable thermogelling chitosan–inorganic phosphate solutions for biomedical applications. Biomacromolecules. 2007;8(12):3779–85.
30. Schussler S, Uske K, Marwah P, Kemp F, Bogden J, Lin S, *et al*. Controlled release of vanadium from a composite scaffold stimulates mesenchymal stem cell osteochondrogenesis. AAPS J. 2017;19(4):1017–28.
31. Gao C, Wei D, Yang H, Chen T, Yang L. Nanotechnology for treating osteoporotic vertebral fractures. Int J Nanomedicine. 2015;10:5139.
32. Cao L, Werkmeister JA, Wang J, Glattauer V, McLean KM, Liu C. Bone regeneration using photocrosslinked hydrogel incorporating rhBMP-2 loaded 2-N, 6-O-sulfated chitosan nanoparticles. Biomaterials. 2014;35(9):2730–42.
33. Mirahmadi F, Tafazzoli-Shadpour M, Shokrgozar MA, Bonakdar S. Enhanced mechanical properties of thermosensitive chitosan hydrogel by silk fibers for cartilage tissue engineering. Mater Sci Eng C. 2013;33(8):4786–94.
34. Townsend JM, Dennis SC, Whitlow J, Feng Y, Wang J, Andrews B, *et al*. Colloidal gels with extracellular matrix particles and growth factors for bone regeneration in critical size rat calvarial defects. AAPS J. 2017;19(3):703–11.
35. Bourke SL, Al-Khalili M, Briggs T, Michniak BB, Kohn J, Poole-Warren LA. A photo-crosslinked poly (vinyl alcohol) hydrogel growth factor release vehicle for wound healing applications. Aaps Pharmsci. 2003;5(4):101–11.
36. Kuo CK, Ma PX. Ionically crosslinked alginate hydrogels as scaffolds for tissue engineering: part 1. Structure, gelation rate and mechanical properties. Biomaterials. 2001;22(6):511–21.
37. Weber LM, Lopez CG, Anseth KS. Effects of PEG hydrogel crosslinking density on protein diffusion and encapsulated islet survival and function. J Biomed Mater Res A. 2009;90(3):720–9.
38. Lawrence PG, Patil PS, Leipzig ND, Lapitsky Y. Ionically cross-linked polymer networks for the multiple-month release of small molecules. ACS Appl Mater Interfaces. 2016;8(7):4323–35.
39. Maitra J, Shukla VK. Cross-linking in hydrogels-a review. Am J Polymer Sci. 2014;4(2):25–31.
40. Zhu Q, Barney CW, Erk KA. Effect of ionic crosslinking on the swelling and mechanical response of model superabsorbent polymer hydrogels for internally cured concrete. Mater Struct. 2015;48(7):2261–76.
41. Ahmed EM. Hydrogel: preparation, characterization, and applications: a review. J Adv Res. 2015;6(2):105–21.
42. Sampath UTM, Ching YC, Chuah CH, Singh R, Lin P-C. Preparation and characterization of nanocellulose reinforced semi-interpenetrating polymer network of chitosan hydrogel. Cellulose. 2017;24(5):2215–28.
43. Moglia RS, Whitely M, Dhavalikar P, Robinson J, Pearce H, Brooks M, *et al*. Injectable polymerized high internal phase emulsions with rapid in situ curing. Biomacromolecules. 2014;15(8):2870–8.
44. Kim H-W, Knowles JC, Kim H-E. Hydroxyapatite/poly (ε-caprolactone) composite coatings on hydroxyapatite porous bone scaffold for drug delivery. Biomaterials. 2004;25(7–8):1279–87.
45. Juhasz JA, Best SM, Bonfield W. Preparation of novel bioactive nano-calcium phosphate–hydrogel composites. Sci Technol Adv Mater. 2010;11(1):014103.
46. Rezwan K, Chen Q, Blaker J, Boccaccini AR. Biodegradable and bioactive porous polymer/inorganic composite scaffolds for bone tissue engineering. Biomaterials. 2006;27(18):3413–31.
47. Mickiewicz RA, Mayes AM, Knaack D. Polymer–calcium phosphate cement composites for bone substitutes. J Biomed Mater Res. 2002;61(4):581–92.
48. O'Donnell JN, Schumacher GE, Antonucci JM, Skrtic D. Structure-composition-property relationships in polymeric amorphous calcium phosphate-based dental composites. Materials. 2009;2(4):1929–54.
49. Okay O, Durmaz S. Charge density dependence of elastic modulus of strong polyelectrolyte hydrogels. Polymer. 2002;43(4):1215–21.
50. Mehmanparast H, Mac-Thiong J, Petit Y. Compressive properties of a synthetic bone substitute for vertebral cancellous bone. Int J Med Biol Sci. 2012;65:287–90.
51. Cesar R, Leivas TP, Pereira CAM, Boffa RS, Guarniero R, Reiff RBM, *et al*. Axial compressive strength of human vertebrae trabecular bones classified as normal, osteopenic and osteoporotic by quantitative ultrasonometry of calcaneus. Res Biomed Eng. 2017;33(2):91–6.
52. Kean T, Thanou M. Biodegradation, biodistribution and toxicity of chitosan. Adv Drug Deliv Rev. 2010;62(1):3–11.
53. Hidaka Y, Ito M, Mori K, Yagasaki H, Kafrawy A. Histopathological and immunohistochemical studies of membranes of deacetylated chitin derivatives implanted over rat calvaria. J Biomed Mater Res. 1999;46(3):418–23.
54. Sarbon N, Sandanamsamy S, Kamaruzaman S, Ahmad F. Chitosan extracted from mud crab (Scylla olivicea) shells: physicochemical and antioxidant properties. J Food Sci Technol. 2015;52(7):4266–75.

55. Caliari SR, Burdick JA. A practical guide to hydrogels for cell culture. Nat Methods. 2016;13(5):405–14.
56. Aguado BA, Mulyasasmita W, Su J, Lampe KJ, Heilshorn SC. Improving viability of stem cells during syringe needle flow through the design of hydrogel cell carriers. Tissue Eng A. 2011;18(7–8):806–15.
57. Zhang Z, Lai Q, Li Y, Xu C, Tang X, Ci J, *et al*. Acidic pH environment induces autophagy in osteoblasts. Sci Rep. 2017;7:46161.
58. Wang J, Witte F, Xi T, Zheng Y, Yang K, Yang Y, *et al*. Recommendation for modifying current cytotoxicity testing standards for biodegradable magnesium-based materials. Acta Biomater. 2015;21:237–49.
59. Schuster SM, Olson MS. The regulation of pyruvate dehydrogenase in isolated beef heart mitochondria. The role of calcium, magnesium, and permeant anions. J Biol Chem. 1974;249(22):7159–65.
60. Denton RM. Regulation of mitochondrial dehydrogenases by calcium ions. Biochim Biophys Acta. 2009;1787(11):1309–16.